

Milad Eyvazi Hesar, Walid Madhat Munief, Achim Müller, Nikhil Ponon, Sven Ingebrandt* Decomposition and modeling of signal shapes of single point cardiac monitoring

Abstract:

We introduce a novel method for electronic recording of cardiac signals from a single point at the skin in contrast to classical differential electrocardiography (ECG). Ultralow-noise transistor devices with an adaptable, auto-stabilizing transimpedance amplifier are able to measure tiny skin potential modulations from a single contact electrode located at an individual's wrist (single-point cardiography-SPC). Although SPC signals were highly prone to interspersed noise, they contained periodic patterns. In an electromagnetically shielded setting, we could clearly extract breathing and cardiac rhythms from the acquired SPC signals. As the reference, we measured ECG in parallel. Several signal-processing techniques like smoothening, correlation, decomposition and signal extraction showed that SPC signals contain breathing and periodic heart potential variations, which are time-correlated with ECG. In the future, we intend to use this novel technique to measure heart signals from patients in different health conditions.

Keywords: Hodrick-Prescott decomposition, ARIMA, STL, Signal Decomposition, AlGaIn/GaN HEMT.

<https://doi.org/10.1515/cdbme-2020-3149>

1 Introduction

Measuring the heart activity is one of the first tests in the clinics. In modern personalized healthcare, different wearable devices were introduced for cardiac monitoring. Healthy people monitor their heart functionality at home, during their daily routines or sports. Most of the approved systems in the

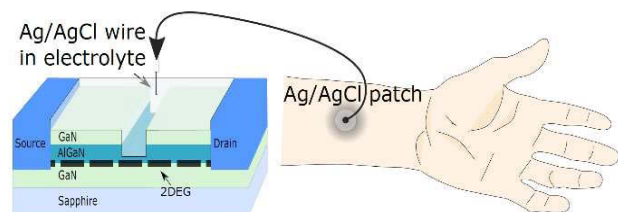


Figure 1. Illustration of a low-noise high electron mobility transistor (HEMT) device with recessed gate structure in a floating electrochemical configuration. A standard skin-patch electrode as it is usually used for ECG was connected via an electrochemical bridge to the transistor.

market, including skin patches, textile-embedded electrodes and smart watches, utilize a classical differential measurement by at least two electrodes like in classical ECG.

In the modern trend of miniaturization and digitalization, wearable devices have attracted high attention. Depending on the level of their precision, there are different methods available: 12-lead ECG, photoplethysmography (PPG), etc. There is always a trade-off between precision and comfortability. More measuring points lead to more precise medical diagnostics with the cost of lower comfortability. For decades, portable 12-lead ECG is measured by the Holter method [1]. Although this method is precise, it has several drawbacks. The high number of electrodes increases the possibility to catch artefacts and noise by body movement and environment [2]. There are also cardiac diseases such as hidden heart attacks, blockage of the arteries, undiagnosed congenital heart defects, myocardial infarction or cardiac scars [3], which are difficult to identify in ECG traces. False positive results were also reported for athletes in their ECG recordings [4]. Since SPC is using only one single point at the wrist to measure the signal, the probability of catching artefacts from multiple points decreases drastically by decreasing the wirings. In many wearable sports and fitness applications, the heart rate is monitored by optical techniques such as PPG. In many biomedical applications, routine electronic monitoring of the heart activity is in high demand for early diagnostics, where SPC might be a valuable complementary technique to ECG.

In this study, we utilized pre-processing, correlation and decomposition methods based on Hodrick-Prescott

*Corresponding author: **Sven Ingebrandt**: RWTH Aachen University, Institute of Materials in Electrical Engineering 1 (IWE1), Sommerfeldstr. 24, Aachen, Germany, e-mail: ingebrandt@iwe1.rwth-aachen.de

Milad Eyvazi Hesar: RWTH Aachen University, IWE1, Aachen, Germany

Walid Madhat Munief, Achim Müller, Nikhil Ponon: RAM Group DE GmbH, Zweibrücken, Germany

60 decomposition, Autoregression Integrated Moving Average
 61 (ARIMA) and Seasonal and Trend decomposition using
 62 Loess (STL) for signal decomposition and correlation of the
 63 recorded SPC traces. Figure 1 shows the experimental setup
 64 using a single patch electrode to contact the test persons’
 65 wrist. The ultralow-noise HEMT transistors in combination
 66 with the battery-powered amplifier pick up tiny fluctuations,
 67 which are not visible with bare skin electrodes and standard
 68 amplifier electronics.

69 2 Methods

70 2.1 Sensors and measurements

71 For SPC recordings, we used ultralow-noise devices
 72 based on AlGaIn/GaN HEMTs [5] in a liquid-gate
 73 configuration [6] to capture tiny fluctuations at a single point
 74 of the skin. A standard Ag/AgCl skin patch electrode was
 75 connected to the wrist of a healthy individual and the lead
 76 attached to another Ag/AgCl wire, which connected an
 77 electrolyte solution. This solution formed a contact to an
 78 electrolyte-gated HEMT transistor (figure 1). HEMTs with
 79 recessed, non-metallized gates were used to increase their
 80 sensitivity [7]. The well-known, ultralow-noise level in
 81 combination with high-ohmic gate inputs of the 2-
 82 dimensional electron gas devices enable the detection of tiny
 83 skin potential fluctuations. With our adaptable, auto-
 84 stabilizing trans-impedance amplifier circuit with floating
 85 gate HEMTs, we generally cannot specify a precise
 86 amplification gain. Depending on the HEMT working point,
 87 the full amplification factor is varying. In SPC detection, the
 88 transistor current changes when a moving charge is
 89 influencing the electrochemical double layer at the input of
 90 the transistor. The amplifier automatically adapts to an
 91 appropriate gain factor to keep the output voltage always in a
 92 similar range. This switching procedure leads to sudden
 93 changes in the output signal. However, for the SPC signal
 94 analysis in this study, we only used recording periods with
 95 coarse trends as it can be seen in figure 2. In addition, since
 96 the measurements were highly prone to interspersed
 97 electromagnetic noise, we did all measurements with test
 98 persons inside a large Faraday tent (Holland Shielding
 99 Systems BV, the Netherlands). In our experiments, we
 100 measured classical ECG signals from the same individual,
 101 simultaneously, to directly correlate the remaining periodic
 102 fluctuations in SPC with ECG, which can also be used to
 103 derive the respiration rate [8]. Experiments were done on six
 104 different individuals sitting on the same chair inside the
 105 Faraday tent, while the battery-powered electronic readout

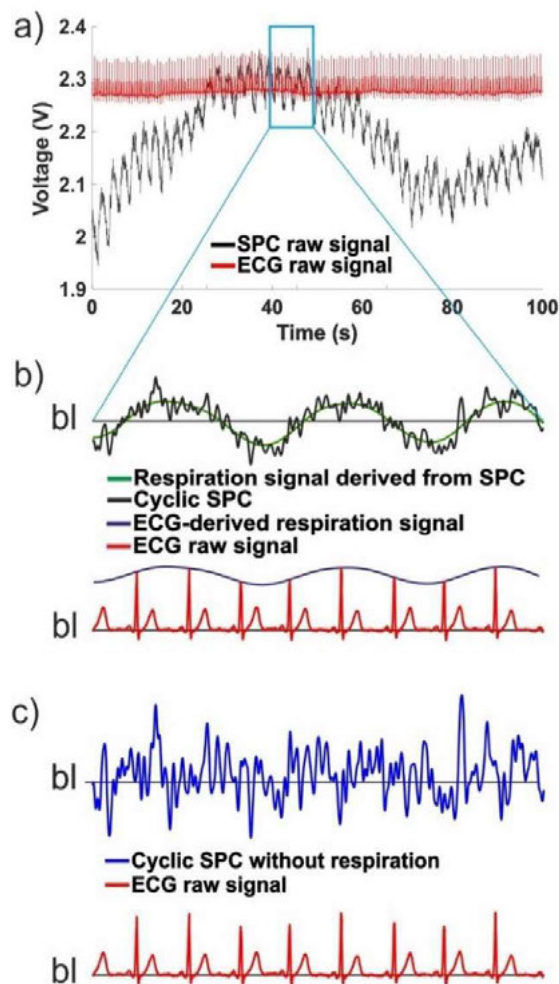


Figure 2. Overview of SPC and ECG traces in the data pre-processing procedure: a) Synchronously recorded ECG and SPC raw data using our multifunctional, battery-powered amplifier unit. b) Raw data ECG signal (red) and ECG-derived respiration modulation (blue). The remaining cyclic component of the SPC signal after the first application of the Hodrick-Prescott filter (black) and the respiration signal derived from SPC (green). It can be seen, that both breathing patterns match each other. c) Cyclic component of the SPC signal subtracted by the respiration modulation. This remaining part of the SPC is subjected to further analysis as core of this study. All filtered and processed data is shown in arbitrary voltage units (bl: baseline)

was acquiring the skin potential fluctuations as shown in figure 1.

2.2 Signal processing

Since SPC signals are time series recordings including floating signals with distinct trends and cyclic fluctuations, we found linear models useful to extract the basic trends in the recordings. We used a Hodrick-Prescott decomposition algorithm to pre-process the SPC signals in order to remove coarse trends [9].

Equation 1 shows a mathematical expression of this filtering technique: The decomposition method is relating two terms of a linear model to decompose the trend and the cyclic parts. In eq. 1 and eq. 2, y_t is the logarithm of the signal, c_t is the cyclic component, τ_t is the trend component and ϵ_t denotes the error. λ defines the weight of the trend and the cyclic parts. We assume, without loss of generality, that the heart of a person is functioning repetitively in any

$$\min_{\tau} \left(\sum_{t=1}^T (y_t - \tau_t)^2 + \lambda \sum_{t=2}^{T-1} [(\tau_{t+1} - \tau_t) - (\tau_t - \tau_{t-1})]^2 \right) \quad (\text{eq. 1})$$

$$y_t = \tau_t + c_t + \epsilon_t \quad (\text{eq. 2})$$

environment. Therefore, the remaining cyclic part of the SPC signal after subtraction of the respiration modulation is supposed to correlate to the heart as the largest muscle in the body. In this respect, the next step in the signal processing was to use suitable mathematical models to extract the most cyclic parts of the signal. Seasonal ARIMA (SARIMA) models are usually denoted as ARIMA(p,d,q)(P,D,Q)_m, where m refers to the number of samples in each season, and the uppercase P,D,Q refer to the seasonal and lowercase p,d,q refer to non-seasonal autoregressive, differencing, and moving average terms for the ARIMA model, respectively.

STL is also widely used as a versatile and robust method for decomposing time series. In this method, Loess is used to estimate nonlinear relationships [10]. In this study we used an Error, Trend, Seasonal (ETS) model with the (A,N,N) configuration. Different criteria such as Akaike's Information Criterion (AIC), Akaike's Information Criterion correction (AICc) and Bayesian Information Criterion (BIC) were used to select the best model. We chose the AICc to evaluate in both of the ARIMA and STL models [11].

3 Results

Since the ultralow-noise HEMT device was operated in a floating gate configuration, the SPC raw data contained coarse trends. These trends were cancelled from the data by signal pre-processing. A first important result of our SPC analysis is that the breathing pattern of a person can be recorded by our technique electronically with only a single skin contact at the wrist. This was already discussed in figure 2 in the signal pre-processing section. We did experiments holding breath or breathing faster, which all correlated to the ECG-derived breathing rhythms as well.

After filtering the strongest cyclic part from the SPC recordings, we assumed that the remaining dominant cyclic signal is most likely time-correlated with the heart rhythm. A Hodrick-Prescott filter with $\lambda = 1600$ was applied to remove

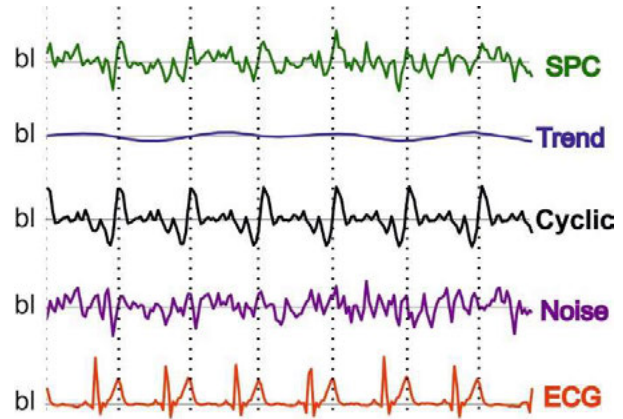


Figure 3. Signal decomposition based on the STL method. After breathing extraction, the remaining trend was very small. The cyclic part of SPC could separate from remaining noise. The cyclic pattern of SPC can be clearly time-correlated with ECG. The y-axis denotes arbitrary voltage units due to signal processing. (bl: baseline)

the coarse trend from the signals. The remaining part contains the breathing signal, the heart signal and remaining noise. Since the frequency of the breathing signal was low (1-3 Hz) in comparison to the heart signal, another additional Hodrick-Prescott filter with the much higher $\lambda \approx 10^{10}$ was applied for extraction of the breathing signal as it was already discussed in figure 2. In figure 3 it can be seen that applying the Hodrick-Prescott filtering was not 100% efficient, since a small trend was still visible as remaining baseline fluctuation correlating with breathing.

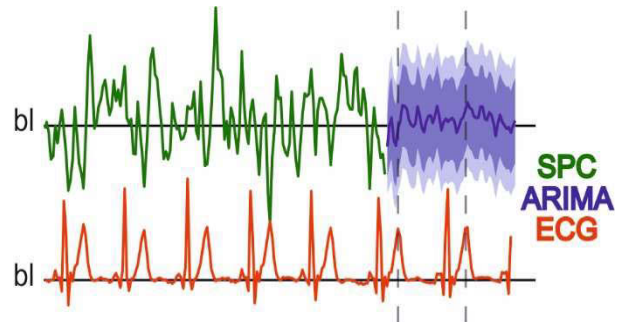


Figure 4. Overlay of the simultaneously measured ECG and SPC traces and a forecasted SPC based on the ARIMA algorithm. (bl: baseline)

Further, applying the STL method separated cyclic components and remaining noise. This noise showed normal distribution and no pattern in the ACFs. Therefore, it should mainly represent transistor and electronic noise. After decomposition, the remaining cyclic SPC trace from STL decomposition showed a clear correlation to the waveform of ECG, which is displayed in the Cyclic and the ECG traces in figure 3. Vertical dashed lines were added as guide for the eyes.

177 After obtaining the general waveform, we overlaid 219
 178 samples of 12 periods of both ECG and pre-processed SPC. 220
 179 Optimizing the autocorrelation factors (ACF), gave 221
 180 ARIMA(0,0,1)(0,0,5)₂₉ (a non-zero mean). The result of the 222
 181 remainder showed no pattern in ACFs. Therefore, we can 223
 182 regard the remaining part as the noise in the measurement. In 224
 183 figure 4, we can see the forecasted signal for the same time 225
 184 needed for one ECG cycle. The optimized ARIMA model is 226
 185 showing actually a moving average filter for both seasonal 227
 186 and non-seasonal terms. 228

187 Therefore, we can regard this remaining part as the noise 229
 188 in the measurement. The Box Cox transformation coefficient 230
 189 was 0.9738, which means this is nearly an additive 231
 190 decomposition. Other coefficients were calculated as AIC=- 232
 191 2354.24, AICc=-2353.82, BIC=-2323.42. In this case, we 233
 192 selected the best model by selecting the minimum AICc,
 193 which shows the minimum loss of data, therefore the highest
 194 quality of the model. The STL model used a Box Cox 234
 195 transformation coefficient, and seasonal window of 12 cycles
 196 for 29 samples per each cycle. 235

197 4 Conclusion

198 We introduce a novel method for the electronic recording 241
 199 of the heart activity by detecting tiny charge fluctuations at a 242
 200 single point of the skin of a person's wrist. With ultralow- 243
 201 noise devices and an auto-stabilizing transimpedance 244
 202 amplifier circuit, we were able to record periodic signals. 245
 203 Skin-charge modulations might stem from charged objects 246
 204 moving and from action of the heart muscle like in ECG. Our 247
 205 data analysis showed that the strongest cyclic components in 248
 206 the SPC traces could be clearly correlated to respiration. After 249
 207 removing the breathing patterns, the remaining SPC signals 251
 208 were strongly time-correlated to the waveforms of 252
 209 simultaneous ECG recordings. 253

210 Heart and lungs are the dominant charge modulating 254
 211 objects in the body. In our experiments, the strongest SPC 255
 212 signal pattern was identified as breathing, because the chest is 256
 213 acting as a large charged and periodically moving object. 257
 214 Furthermore, the strongest part of the remaining SPC traces 258
 215 correlated to the ECG T-wave, which reflects the 259
 216 repolarization of the ventricles (figure 4). At this state of the 260
 217 heart cycle, ventricles, the strongest muscle components of 261
 218 the heart, stretch and relax. 263

In the future, we aim to interpret the SPC signals with
 respect to an electrical and mechanical heart activity to
 understand the signal shapes and to identify potentially
 healthy from diseased conditions in patients.

The novel SPC technique as introduced here might
 complement the classical ECG techniques of cardiac
 monitoring in future healthcare.

Author Statement

Research funding: Funding came from the BMBF KMU-
 innovative project 'Einzelpunkt-Sensorsystem für die nicht-
 invasive, dynamische Messung der Herzfunktion'
 (SINDynamik - FKZ: 13GW0180B).

Conflict of interest: The authors declare the existence of a
 financial competing interest.

References

1. Holter, N.J., *New Method for Heart Studies - Continuous Electrocardiography of Active Subjects over Long Periods Is Now Practical*. Science, 1961. **134**(348): p. 1214-&.
2. Everss-Villalba, E., et al., *Noise Maps for Quantitative and Clinical Severity Towards Long-Term ECG Monitoring*. Sensors, 2017. **17**(11).
3. Turkbey, E.B., et al., *Prevalence and Correlates of Myocardial Scar in a US Cohort*. JAMA, 2015. **314**(18): p. 1945-54.
4. *ECG Limitations*. JAMA, 2000. **284**(6): p. 686-686.
5. Ambacher, O., et al., *Two-dimensional electron gases induced by spontaneous and piezoelectric polarization charges in N- and Ga-face AlGaIn/GaN heterostructures*. Journal of Applied Physics, 1999. **85**(6): p. 3222-3233.
6. Steinhoff, G., et al., *pH response of GaN surfaces and its application for pH-sensitive field-effect transistors*. Applied Physics Letters, 2003. **83**(1): p. 177-179.
7. Vitushinsky, R., et al., *Enhanced detection of NO₂ with recessed AlGaIn/GaN open gate structures*. Applied Physics Letters, 2013. **102**(17): p. 4.
8. Widjaja, D., et al., *ECG-Derived Respiration: Comparison and New Measures for Respiratory Variability*. Computing in Cardiology 2010, Vol 37, 2010. **37**: p. 149-152.
9. Hodrick, R.J., *An Exploration of Trend-Cycle Decomposition Methodologies in Simulated Data*. 2020, National Bureau of Economic Research.
10. Cleveland, R.B., *STL: A seasonal-trend decomposition procedure based on loess*. 1990. DOI: citeulike-article-id. **1435502**.
11. Oller, L.E. and P. Stockhammar, *Forecasting with Exponential Smoothing: The State Space Approach*. International Journal of Forecasting, 2010. **26**(1): p. 204-205.